

Glitch in Time: Exploiting Temporal Misalignment of IMU For Eavesdropping

Ahmed Najeeb

LUMS

Pakistan

Naveed Anwar Bhatti

LUMS

Pakistan

Abdul Rafay

LUMS

Pakistan

Muhammad Hamad Alizai

LUMS

Pakistan

Abstract

The increasing use of voice assistants and related applications has raised significant concerns about the security of Inertial Measurement Units (IMUs) in smartphones. These devices are vulnerable to acoustic eavesdropping attacks, jeopardizing user privacy. In response, Google imposed a rate limit of 200 Hz on permission-free access to IMUs, aiming to neutralize such side-channel attacks. Our research introduces a novel exploit, *STAG*, which circumvents these protections. It induces a temporal misalignment between the gyroscope and accelerometer, cleverly combining their data to resample at higher rates and reviving the potential for eavesdropping attacks previously curtailed by Google's security enhancements. Compared to prior methods, *STAG* achieves an 83.4% reduction in word error rate, highlighting its effectiveness in exploiting IMU data under restricted access and emphasizing the persistent security risks associated with these sensors.

1 Introduction

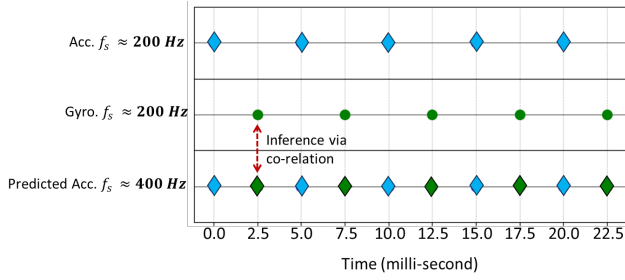
Smartphones' Inertial Measurement Units (IMUs), comprising accelerometers and gyroscopes, are vulnerable to eavesdropping attacks that exploit their capacity to detect vibrations from human speech [4, 5, 21, 23, 36]. While earlier studies focused on reconstructing human voice signals, which would require capturing the entire audio spectrum up to 40 kHz, recent advancements emphasize recognizing patterns within the captured data.

Reconstruction, requiring high-frequency data, aims to recreate the original audio signal, whereas *recognition* focuses on identifying specific speech patterns or features achievable with lower-frequency data. The voiced speech of an adult male typically has a fundamental frequency of 85 to 180 Hz, while that of an adult female ranges from 165 to 255 Hz [24]. These frequencies fall within the lower range of human speech and can be partially captured by smartphone motion sensors. Despite their limited sampling rate, which typically goes up to 600 Hz, these sensors are capable of detecting key low-frequency speech features, making them a potential target for eavesdropping attacks. Understanding these frequency ranges is crucial, as it underscores the risk that even low-frequency components of speech can be exploited, especially given

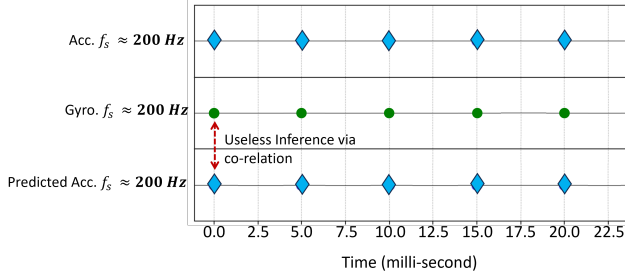
that fundamental speech frequencies are within the detection capabilities of IMUs.

Earlier efforts like Accessory [23] and Gyrophone [21] assessed the feasibility of these attacks, albeit with limited accuracy. Subsequent developments, such as Spearphone [5], Accelword [36], Speechless [4], and StealthyIMU [29], capitalized on the proximity of IMUs to smartphones' loudspeakers, improving the effectiveness of attacks. Nonetheless, security enhancements in Android 12 [16], which restrict IMU sampling to 200 Hz and require user permission for higher rates, have effectively mitigated many of these zero-permission attack strategies. The reduction of the permission-free zone to 200 Hz has effectively eliminated the majority of low-frequency components, thereby leaving an insufficient amount of information for developing effective recognition systems, which is exceedingly challenging under these constraints. This reflects the dynamic interplay of evolving threats and countermeasures in smartphone security.

We introduce **Sensor Fusion via Temporal Misalignment in Accelerometers and Gyroscopes (*STAG*)**, a novel approach that effectively circumvents the 200 Hz sampling rate limitation in modern smartphones. A critical aspect of our research is the introduction of controlled temporal misalignment between accelerometer and gyroscope readings, a technique that reestablishes the eavesdropping threat posed by IMUs. This misalignment leverages the established correlation [34, 35] between these data types to enhance accelerometer data upscaling. By deliberately avoiding the synchronization of sensor readings, we prevent data overlap and significantly enhance the accuracy of data fusion. Under conditions where a 200 Hz sampling rate is utilized without special permissions, a temporal misalignment of approximately 2.5 ms between the gyroscope and accelerometer enables the reconstruction of an upsampled 400 Hz signal. This 2.5 ms misalignment is strategically set at the midpoint between two consecutive accelerometer samples, as shown in Figure 1a. The intentional deviation from standard sensor operation, where accelerometer and gyroscope data are typically aligned in time, distinguishes our method from conventional sensor fusion techniques, as illustrated in Figure 1b.



(a) Illustration of optimal temporal misalignment in IMU sensors.



(b) Standard alignment in conventional IMU sensor configurations.

Figure 1. Data sampling of IMU sensors: contrasting optimal temporal misalignment vs. standard alignment in smartphones.

We have devised a sophisticated data processing pipeline to upscale accelerometer data, incorporating gradient boosting [8] and interpolation [11]. This integration markedly enhances the precision of upsampled data by intelligently combining it with temporally misaligned gyroscope readings. Our method exceeds the performance of existing 200 Hz techniques like InertiEAR [14] and StealthyIMU [29]. Unlike InertiEAR, which only recognizes predefined words, our approach supports continuous speech recognition—a significant functional enhancement. Moreover, our method records a dramatically lower Word Error Rate (WER) of **13%** compared to StealthyIMU's **78.75%**, demonstrating superior accuracy in complex speech recognition at reduced sampling rates. This accomplishment represents a significant step forward in understanding zero-permission voice eavesdropping and draws attention to an important security concern in smartphone operating systems. Addressing this vulnerability will strengthen the overall security and safety of Android users, much like how previous efforts to resolve security issues have benefited the broader community.

We make the following contributions:

[C1] Demonstrating inadequacy of existing security measures: Our research demonstrates that the 200 Hz sampling rate restriction introduced in Android 12 and later versions is inadequate for preventing sophisticated eavesdropping attacks via motion sensors, necessitating a comprehensive reevaluation of security criteria for sensor data in smartphones.

[C2] Temporal misalignment technique: We have developed a novel method to induce controlled temporal misalignment in IMU data. This technique strategically adjusts the synchronization between accelerometer and gyroscope readings, which enhances the precision of data fusion processes. It significantly improves the upscaling of accelerometer data from 200 Hz to 400 Hz.

[C3] Upscaling pipeline: We have introduced an advanced data processing pipeline that innovatively integrates the Light Gradient Boosting Machine (LightGBM) with interpolation. This approach is tailored to improve audio signal recognition through IMU data, significantly enhancing the accuracy and efficiency of audio recognition at reduced sampling rates.

2 Preliminaries

We present a fundamental overview of key concepts and the current state of research pertinent to our study. This overview encompasses an examination of MEMS sensors, specifically accelerometers and gyroscopes, a comprehensive review of Gradient Boosting Machines and Sensor Fusion techniques, and an analysis of recent advancements in Spoken Language Understanding. Through this exploration, we lay the theoretical foundation for our research and contextualize our contributions within the landscape of ongoing developments in these areas.

2.1 Background

We explore the technical details that play distinct and interrelated roles in advancing our research objectives.

2.1.1 MEMS Sensors: Smartphones are typically equipped with both a three-axis accelerometer and a three-axis gyroscope, which are MEMS [20, 27]. These sensors are essential for detecting device motion, orientation, vibration, and shock. The accelerometer measures acceleration on three axes using a seismic mass, fixed electrodes, and springs. Movements shift the seismic mass, changing the capacitance between electrodes, and converting into acceleration measurements. This setup also detects mechanical vibrations, interpreting them as acceleration. Similarly, the gyroscope measures angular rates using the Coriolis force [30], with a vibrating mass that moves along two axes. External movements induce a Coriolis force that displaces the mass and alters the capacitance, from which angular rates are calculated. In Android smartphones, motion sensor data can be accessed at sampling rates up to 200 Hz without special permissions and up to 600 Hz with permissions, depending on the device's capabilities.

2.1.2 Gradient Boosting Machines (GBM): These are advanced ensemble learning methods employed in machine learning for regression and classification tasks [22]. These machines iteratively build an ensemble of weak predictive

models, primarily decision trees, to create a robust predictive model. Each subsequent model aims to correct the errors of the previous ones, refining predictions incrementally. The ‘gradient’ in gradient boosting refers to the application of the gradient descent algorithm, which minimizes the model’s error. GBMs are noted for their predictive accuracy, adaptability to various data types, and robustness against overfitting. Our research utilizes LightGBM [19], a GBM variant known for its computational efficiency and minimal memory usage, employing a histogram-based decision tree learning algorithm suitable for limited-resource environments.

2.1.3 Sensor Fusion: It is an advanced data processing technique that combines data from multiple sensors to achieve a more accurate and comprehensive understanding than is possible with individual sensors alone [13, 25, 26]. This technique is critical in applications where integrating diverse data sources is vital to enhanced perception and decision-making. It merges data from accelerometers, gyroscopes, video cameras, and WiFi signals, improving system accuracy and reliability. Sensor fusion is instrumental in navigation systems like Google Maps, where it integrates GPS and sensor data to precisely determine a user’s location and orientation [15]. In our research, we apply sensor fusion principles to effectively combine accelerometer and gyroscope data using gradient boosting, aiming to refine data sets for improved eavesdropping attack models.

2.1.4 Spoken Language Understanding (SLU): Voice assistants must interpret and respond to human speech [33]. SLU processes involve intent detection, classifying spoken phrases according to their purposes, and slot filling, which extracts details like dates and locations from speech. Modern SLU systems may use a cascaded pipeline that first transcribes speech to text before applying Natural Language Understanding (NLU), or an end-to-end model that directly maps speech signals to intents and slots, thereby avoiding transcription errors [29]. Recent advancements have introduced joint models that manage both tasks simultaneously and incorporate pre-trained language models and deep neural networks, significantly enhancing SLU performance. Our study utilizes StealthyIMU [29] SLU as a benchmark, an end-to-end SLU model proficient at extracting sensitive data from motion sensor signals, illustrating this method’s efficacy in utilizing sensor-based data leakage.

2.2 Related Works

Research on speech recognition using motion sensors broadly falls into two categories. The first involves studies on recognizing external voice inputs through smartphone motion sensors. The second focuses on speech recognition from internal sources, typically using the smartphone’s loudspeakers. Table 1 presents a detailed comparison of these studies with our approach, STAG. We assess the accuracy of previous methods based on non-permission IMU data sampled below

200 Hz. We further show evaluation metrics used and whether the papers use constrained or unconstrained data. Constrained, in our case, means that the data used is based on a limited set of digits or words, while unconstrained means that the Model can account for unseen vocabulary.

Gyrophone [21] investigates a smartphone placed near a loudspeaker on a solid surface. Using the gyroscope, it detects speech signals from the external loudspeaker for speech recognition and speaker identification. However, the gyroscope’s limited sensitivity to surface vibrations and its 200 Hz sampling rate cap pose challenges in achieving high accuracy in recognition tasks.

AccelWorld [36] explores scenarios where a user speaks near a smartphone, either handheld or on a desk. The accelerometer captures speech signals through air transmission, aiding in hot word detection like “Okay, Google” or “Hi, Galaxy.” PitchIn [17] uses a distributed time-integrated analog-digital conversion (TIADC) system to approximate high sampling frequencies with low per-node rates. By pooling data from multiple devices, PitchIn demonstrates effective speech recognition, showcasing the potential of eavesdropping through closely-placed devices.

These initial methods primarily utilized external human speech. A more concerning attack vector involves the smartphone’s built-in loudspeaker. Since the motion sensors are physically close to the speaker within the same device, they pose a higher risk of revealing sensitive information during calls or voice assistant interactions. Background applications can exploit zero-permission motion sensors to capture and reconstruct this data.

AccelEve [9] marks the first study exploiting loudspeaker proximity to Inertial Measurement Units (IMUs). It employs a deep learning model (DenseNet) to reconstruct speech from accelerometer signal spectrograms, achieving a top-1 accuracy of 78% for digits and 55% for digits plus letters. Spearphone [5] utilizes altered accelerometer readings and machine learning techniques to classify gender with over 90% accuracy and identify speakers with over 80% accuracy. Additionally, Spearphone can reconstruct speech with a word detection accuracy of 67%.

AccEar [18] expands the scope to include a wider range of vocabulary. Using a conditional Generative Adversarial Network (cGAN), AccEar enhances spectrograms from low-frequency accelerometer signals to reconstruct high-fidelity audio, achieving 90% accuracy under optimal conditions. StealthyIMU [29] extends this to voice assistants, accessing sensitive information like GPS and contact data via an accelerometer. It formulates this side-channel attack as an end-to-end private speech understanding challenge, using Sentence Error Rate (SER) as the metric. SER considers a response to be error-free only if all entities in a single voice assistant response are correctly identified. StealthyIMU reaches an 86% sentence accuracy (1-SER) and 37% without permission

Table 1. Overview of related work

Paper	Sensor	Recognition	Evaluation Metric	Accuracy @ 200 Hz
Gyrophone [21]	Gyro	Digits (constrained)	Accuracy	17%
Accelword [36]	Acc	Words (constrained)	F-measure	85%
PitchIn [17]	Acc	Words (constrained)	Accuracy	NA
Spearphone [5]	Acc	Digits + Words (constrained)	F-measure	NA
AccelEve [9]	Acc	Digits + Letters (constrained)	Accuracy	NA
AccEar [18]	Acc	Words (unconstrained)	1-WER	NA
InertiEar [14]	Acc+Gyro	Digits + Letters (constrained)	Accuracy	78.8%
StealthyIMU [29]	Acc	Spoken Language Understanding (unconstrained)	1-SER 1-WER	37% 21.25%
STAG [Ours]	Acc+Gyro	Spoken Language Understanding (unconstrained)	1-SER 1-WER	58% 86.98%

access, although our evaluation shows a significantly lower sentence detection accuracy.

Google’s sampling rate restrictions have limited the effectiveness of these methods, with most underperforming below 200 Hz. InertiEar [14] attempts to circumvent this by using IMUs to eavesdrop on both top and bottom smartphone speakers. By exploiting the coherence between accelerometer and gyroscope responses and their hardware diversity, InertiEar achieves a greater than 75% speech recognition accuracy for digits and letters.

Our study diverges from the existing literature in two crucial aspects. First, we address the sampling rate issue by upsampling the accelerometer signal, thereby enhancing the input quality for existing models. Second, we introduce a novel method to induce perfect temporal misalignment between accelerometer and gyroscope values, maximizing the benefits of data fusion. The closest related work, InertiEar, does not introduce any form of misalignment, which partly explains why our approach achieves higher accuracy (Section 5.3). Our contribution, STAG, functions as an effective preprocessing layer for existing ML models, circumventing Google’s rate limitations and significantly enhancing the effectiveness of previous eavesdropping attacks.

3 Problem Formulation

Our research focuses on uncovering a critical vulnerability in the Android operating system, specifically related to how its scheduler impacts the alignment of sensor data streams. Rather than emphasizing application development, we draw attention to a security weakness in synchronizing Android’s sensor data. Misaligned sensor data streams can be exploited for covert surveillance, posing severe privacy risks. Given Android’s

status as one of the most widely used operating systems, our findings demonstrate how existing security measures—such as the 200 Hz sampling limit—may create a false sense of protection.

3.1 Threat Model

Our research focuses on a typical scenario involving Android smartphone users, who represent a significant segment of the global smartphone market. The relevance of our study is amplified by Android’s recent security update in Android 12 in 2021 [16], which limits the IMU sampling rate to 200 Hz. We examine the potential risks when smartphones broadcast speech signals through their loudspeakers, potentially revealing sensitive personal information. The associated threat escalates due to the extensive permissions often granted to voice assistant applications, such as access to calendar, contacts, location, microphone, phone, SMS, and storage [15], each a potential repository of private data.

Our method, STAG, is designed to harness the potential of zero-permission motion sensors to capture vibrations from various audio sources, including voice assistants and human conversations, even within the constraints of the new sampling rate limits. This is achieved by deliberately inducing temporal misalignment between accelerometer and gyroscope readings. Our threat model envisions a scenario where a user unwittingly installs an app containing STAG. The app could store the harvested data locally or, if permissions allow, upload it to a cloud server for advanced analysis. Popular mobile browsers like Chrome, Brave, and Firefox provide default access to motion sensors without explicit user permission [12]. Thus, in addition to embedding itself in standard applications, malicious software can also be deployed through executable scripts (e.g.,

PyScript, Javascript) on seemingly benign websites, enabling it to process the data locally and surreptitiously upload it to a remote server without the user's knowledge.

3.2 Attack Scenarios

In the scenario of a malicious app installed on a smartphone, the following types of information could be at risk:

- [AS1] **Location information:** The malicious app can use responses from the voice assistant, especially for weather-related queries, to infer the user's coarse location, such as their city or county (city district) of residence. The app can pinpoint the general area where the user is located by analyzing the specific details mentioned in the loudspeaker's output.
- [AS2] **User routine:** The app leverages SLU to decode responses from the voice assistant to user queries. It systematically collects and analyzes this data to detail the user's daily routine. Information from reminders and to-do lists reveals scheduled activities, while queries about directions show regular travel routes and frequented locations. This thorough analysis not only maps typical daily activities but also predicts future behaviors based on recurring patterns.
- [AS3] **Communication sphere:** Voice assistants, which access users' contact lists for initiating calls and sending messages via voice commands, present a privacy risk when exploited by malicious apps. Such apps can covertly listen to interactions to discern contact identities and capture content confirmed verbally by the voice assistant. This unauthorized access to private message contents could lead to substantial privacy breaches.

These scenarios highlight the diverse ways in which a sophisticated malicious app could exploit the functionalities of a smartphone to extract sensitive personal information, underscoring the need for robust security measures.

4 Design and Implementation

STAG has been refined into a robust system capable of augmenting the utility of sensor data for various applications. In the following subsections, we dissect the key components of STAG, detailing the architecture's complexities and the rationale behind each design decision.

4.1 Temporal misalignment

To counteract the challenge posed by Android's 200 Hz sampling rate cap on accelerometer sensors, our research undertook a methodical investigation to acquire or infer missing accelerometer data. This investigation was structured around experimenting with three distinct scenarios, all centered on the concept of *temporal misalignment*—a strategic offset in the timing of different sensor readings. The initial scenarios offered valuable, albeit incremental, insights into the problem.

However, it was the exploration of the final scenario that led to a breakthrough. Each scenario was a step forward in an iterative process, gradually leading us to the successful implementation of temporal misalignment as a viable solution.

4.1.1 Scenario 1: multiple accelerometer instances.

In our initial approach, we implemented two separate software instances of the accelerometer sensor within our Android application. Each was set up to sample at an approximate rate of 200 Hz, with a slight offset in their initialization times. The intention was to merge these sets of data to simulate an effectively higher sampling rate.

However, this method encountered a significant limitation. Despite their staggered start times, both accelerometer instances produced readings with identical timestamps. This outcome was due to both instances drawing data from the same physical accelerometer sensor. As a result, the sensor values, which are dependent on the changes in the sensor's state, were the same for both instances. Moreover, the Android operating system does not guarantee a fixed 200 Hz sampling rate; the actual rate can fluctuate above or below this figure. This rate flexibility allows Android to provide the most recent sensor values to any software instance of the accelerometer. Due to this system behavior and the shared use of the physical sensor, both software instances ended up capturing essentially identical data, as reflected in their synchronized timestamps. **Lesson Learned:** *Attempting to create multiple software instances of the accelerometer within an Android application to simulate a higher sampling rate is ineffective. The Android operating system's handling of sensor data results in identical timestamps for readings from both instances, due to their shared use of the same physical sensor. This highlights the limitations imposed by the OS and hardware design on sensor data manipulation.*

4.1.2 Scenario 2: gyroscope and accelerometer instances.

In our subsequent experiment, we implemented a strategy that involved registering both a gyroscope and an accelerometer in the Android application. Each sensor was configured to sample at approximately 200 Hz, with a deliberately introduced delay in their initiation. However, similar to our first attempt, this method also led to both sensors providing readings with identical timestamps.

The cause of this synchronized timestamp phenomenon can be traced back to two main factors. Firstly, Android's management of sensor sampling rates is inherently flexible; while a maximum rate is specifiable, the actual sampling frequency can vary and is adjusted in real-time by the operating system. This variability in the sampling intervals could result in the gyroscope and accelerometer inadvertently aligning their readings, despite our efforts to stagger their activation. Secondly, the design of IMU sensors, which encompasses both accelerometers and gyroscopes, is inherently inclined towards synchronized functioning. These sensors are typically integrated at both hardware and software levels to facilitate

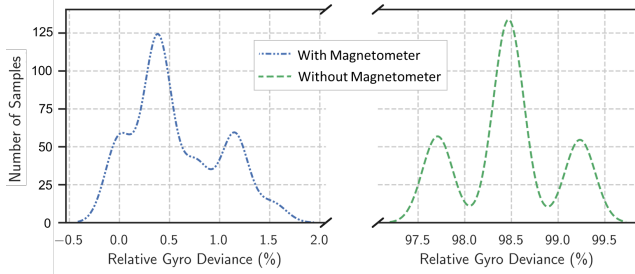


Figure 2. Temporal misalignment and sample distribution in the Samsung Galaxy A33 before and after integrating the magnetometer.

efficient and precise motion detection, which naturally leads to their simultaneous data sampling and reporting. A key finding was the consistent zero variance in sampling delays, indicating potential for precise gyroscope sample alignment in future experiments.

Lesson Learned: *Introducing gyroscope and accelerometer sensors with a staggered initialization also fails to achieve desynchronized readings, as the Android OS manages sensor sampling rates flexibly and IMU sensors are designed to operate synchronously. This experiment underlines the challenge of achieving temporal misalignment through software alone, due to the inherent synchronized functioning of IMU components and the OS's real-time adjustments to sampling rates.*

Table 2. Gyroscope deviation from the ideal central position, with and without magnetometer influence, across various smartphone models.

Device	Gyro deviation from centre (%)	
	No Mag	With Mag
Redmi Note 12	100.0000	100.0000
Samsung Galaxy A73	100.0000	100.0000
ONEPLUS 6T	0.0093	0.0092
Samsung Galaxy A33	98.4629	0.5662
Samsung Galaxy M31	98.7281	0.5797
Google Pixel 5	51.4633	22.9684

4.1.3 Scenario 3: introducing magnetometer. A pivotal discovery emerged during the integration of magnetometer with gyroscope and accelerometer systems: the unexpected desynchronization of their readings, which enhanced the effectiveness of sensor fusion. We achieved the desired misalignment by enforcing consecutive gyroscope and accelerometer readings to be interleaved with magnetometer readings.

The distinct hardware configurations of sensors, particularly the STMicroelectronics LSM6DSM IMU [28] found in the Samsung A31/A33 and the Bosch BMI160 IMU [10] used

in the Pixel 5, involve direct connections between the IMU and the host, with the magnetometer interfacing through the IMU. This architectural design involves a FIFO buffer within the IMU that aids in efficient high-frequency data capture and energy savings. However, it can introduce synchronization problems when integrating a Magnetometer which does not have its own FIFO buffer and whose values are stored in the FIFO of IMU—leading to data misalignments, as our research indicates.

Lesson Learned: *Integrating a magnetometer with gyroscope and accelerometer systems can effectively introduce the desired temporal misalignment, enhancing sensor fusion effectiveness. The distinct hardware configurations, particularly with the magnetometer sensor being the slave to the IMU and the presence of FIFO buffers in IMU devices, contribute to this desynchronization. This scenario reveals the potential for exploiting hardware-level interactions between sensors to achieve precise temporal misalignment, thereby advancing the development of effective recognition systems. However, this also uncovers security vulnerabilities in certain smartphone models, where this misalignment could be exploited for unauthorized data extraction.*

Table 2 classifies devices based on gyroscope deviation from the center, with or without a magnetometer. Devices in red show unchanged deviation; yellow devices, like the ONEPLUS 6T, display minimal deviation; green devices significantly approach the ideal misalignment. Despite optimal alignment at 2.5 ms, data fusion accuracy remains consistent with up to a 25% deviation, demonstrating the complex nature of current smartphone sensor systems. Figure 2 for the Samsung Galaxy A33 illustrates how gyro deviation consolidates into the ‘ideal region’ post-magnetometer integration, emphasizing substantial shifts toward desired misalignment.

These results show that temporal misalignment can be exploited to increase the effective sampling rate. After achieving misalignment between the accelerometer and gyroscope readings, each operating at 200 Hz with a 2.5 ms offset, we successfully doubled the effective sampling rate to 400 Hz. However, further upsampling beyond this limit would only rely on repeating or interpolating existing data, leading to diminishing returns in quality and accuracy. Therefore, our analysis focused on this limit to demonstrate the efficacy of our method within the Android system’s constraints.

4.2 Establishing Correlation

To fully leverage the capabilities of STAG’s temporal misalignment, a critical analysis of both the signal-to-noise ratio (SNR) and the correlation index between accelerometer and gyroscope data is imperative. The SNR provides an indication of the quality of the signal, whereas the correlation index reveals the strength of the relationship between the two data streams, a connection that is not inherently ensured by a high SNR alone.

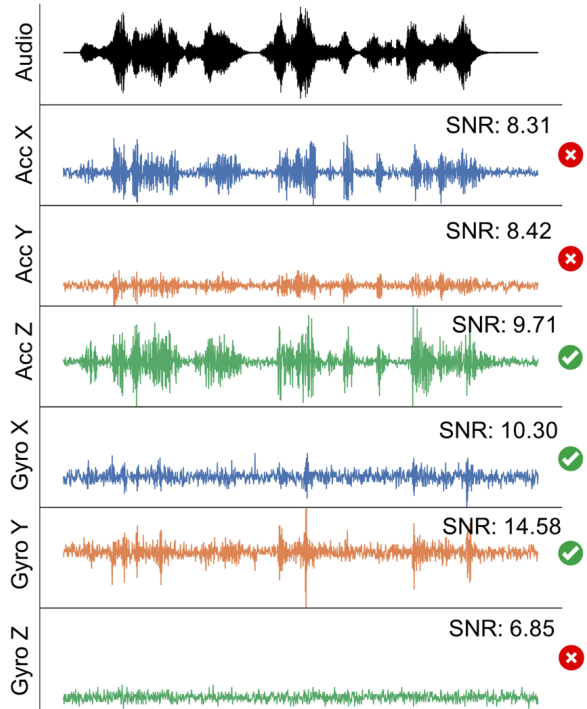


Figure 3. Normalized sensor responses to audio: Gyroscope and accelerometer readings are shown with the y-axis scaled from 0 to 1. The accelerometer exhibits a higher response compared to the gyroscope, yet both display discernible patterns.

For our purposes, the Z-axis of the accelerometer is consistently selected due to its superior SNR, which remains stable across different smartphone positions and varying sound volumes. This stability is primarily attributed to its alignment with the loudspeaker vibrations, as depicted in Figure 3. However, a high SNR in the accelerometer does not automatically imply a strong correlation with the gyroscope’s data. Therefore, assessing the correlation index is equally essential to ascertain that the chosen axes of the gyroscope exhibit a significant relationship with the accelerometer’s Z-axis, a crucial factor for precise data prediction.

Our investigation indicated that while the accelerometer’s Z-axis showcased the highest SNR, it was the X and Y axes of the gyroscope that exhibited the most substantial correlation with the Z-axis of the accelerometer, as evidenced in Figure 4. While this correlation figure is specific to the Samsung Galaxy A33, similar patterns were observed in all the mobiles mentioned in Table 2, reinforcing the generalizability of our findings. This finding implies that, regardless of their SNR, the gyroscope’s measurements on the X and Y axes are effectively correlated with the linear acceleration detected by the accelerometer’s Z-axis. Consequently, these axes become ideal candidates for sensor fusion within the STAG framework.

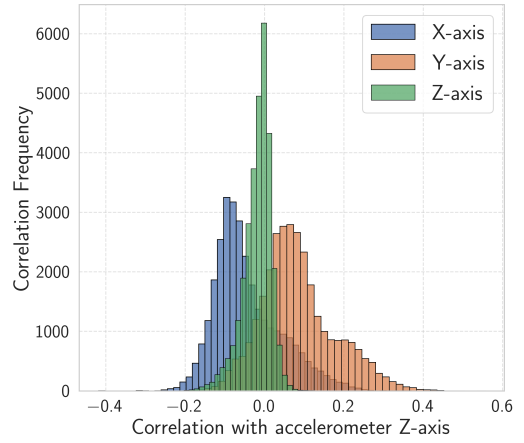


Figure 4. Gyroscope axes correlation with Z-axis of the accelerometer.

In summary, by choosing the accelerometer’s Z-axis for its high SNR and the gyroscope’s X and Y axes for their strong correlation with the accelerometer’s Z-axis, we equip STAG’s machine learning models with data that is of high quality and strongly correlated. This strategic combination of SNR and correlation index is essential in successfully predicting missing accelerometer data and achieving precise sensor fusion in STAG’s architecture.

4.3 Data collection

To enhance the performance of our STAG system in interpreting speech labels, we collected over 16,000 new sensor readings from accelerometers and gyroscopes [7]¹. This was in addition to utilizing 20,000 existing readings from the StealthyIMU dataset [3].

For textual data, we utilized Google’s Directions API to derive travel routes between a combination of over 100 cities and prominent landmarks within the United States, ensuring consistency with the StealthyIMU dataset and aiming to enhance prediction accuracy. The city list was generated using GPT and validated through the Maps API. These routes were converted into spoken instructions using Google’s Text-to-Speech service, which employs the WaveNet model—technology also utilized by Google’s voice assistant [2]. To extract all SLU entities from each route description, we employed SpaCy [1], a Python library for natural language processing, and combined it with regular expression techniques and the GPT-4 API. This rigorous process ensures that our system accurately interprets the speech labels. All collected data, including each wave file and associated metadata, were organized and stored in CSV format.

To collect sensor readings, we designed a simple Android application that retrieves .wav files from a server hosted

¹Reference withheld due to double blind.

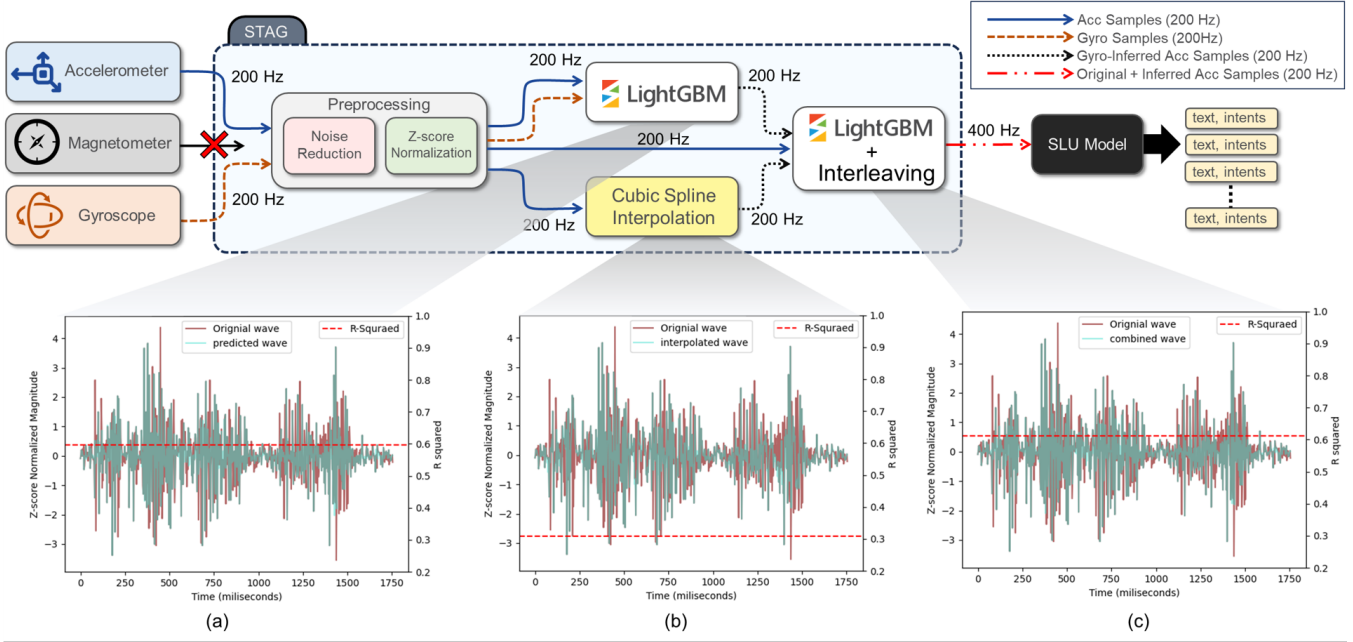


Figure 5. Overview of the STAG Architecture and its Accuracy Assessment: Panel (a) displays the results of predictions made by the LightGBM model on normalized accelerometer data. Panel (b) illustrates the outcome of cubic spline interpolation applied to the data, enhancing resolution for improved analysis. Panel (c) demonstrates the accuracy enhancement achieved through the combination of the original and inferred accelerometer samples, with respective R-squared values indicating the goodness of fit. The overall flowchart depicts the preprocessing steps applied to accelerometer and gyroscope data, followed by feature extraction using LightGBM, interpolation, and final analysis in the SLU model.

on a Raspberry Pi with a static IP. The app plays these audio instructions through a smartphone’s loudspeaker while simultaneously recording data from the accelerometer and gyroscope at a 400 Hz sampling rate. The recorded data is then sent back to the server for storage and analysis. This automated setup not only enables remote real-time data analysis—essential for assessing our system’s efficacy and reducing data transfer delays—but also supports parallel data collection using a client-server model. Each device accesses only the necessary metadata, with audio files centrally stored on the Raspberry Pi. The entire experiment was conducted in a soundproof room and lasted 32 continuous hours.

4.4 Model Selection

The central role of the machine learning model in the STAG system is to upscale the accelerometer data from its native sampling rate of 200 Hz to the desired 400 Hz range. This enhancement in the sampling rate is vital for increasing both the detail and accuracy of the sensor data. Such an improvement significantly augments the system’s acoustic surveillance capabilities, enabling a more precise capture and analysis of sound data, all while operating within the existing permission constraints.

Streaming raw accelerometer and gyroscope data continuously from mobile devices consumes substantial network

resources and increases detection risks. Our initial tests revealed that transmitting unprocessed data for 16 hours resulted in 537.6 MB of data, compared to just 1.2 MB for processed data. To improve efficiency and reduce detection risks, we recommend on-device processing, which considerably lowers bandwidth usage by minimizing the data required for transmission, potentially obviating the need for it entirely.

Table 3. Comparative analysis of machine learning models’ memory overhead vs. efficiency.

Model	Memory Usage (MB)	Inference time (ms)
RNN	1149.4	0.6335
CNN	1081.1	0.6340
Random Forest	957	0.6383
LightGBM	827.7	0.6393

Choosing a machine learning model that requires minimal memory and processing power is essential due to the constrained computational resources and battery life of mobile devices. To identify the optimal model, we evaluated popular algorithms including LSTM, CNN, RNN, Random Forests, and LightGBM, focusing on model complexity, memory usage, processing speed, and accuracy (Table 3). LightGBM

was found to be the most appropriate, offering low memory usage and fast inference times, making it ideal for on-device deployment. Its efficient architecture ensures rapid processing and minimal resource consumption, while its robustness in modeling complex data interactions makes it well-suited for sensor fusion tasks.

4.5 STAG Architecture

The STAG system integrates various findings from our research into a unified architecture that enhances sensor data upsampling through a blend of temporal misalignment, sensor data correlation, and machine learning optimization. Outlined in Figure 5, the architecture involves critical stages of Prediction, Interpolation, and Combination, pivotal for precise sensor fusion.

STAG starts by misaligning accelerometer and gyroscope data sequences, optimizing them through a dual-method up-sampling of LightGBM and cubic spline interpolation, with respective R-squared values shown in Figure 5(a) and (b). Data accuracy is further refined by merging the prediction and interpolation outputs, achieving an enhanced R-squared value depicted in Figure 5(c).

The processed data is utilized by an SLU model to produce predictive text, transforming misaligned sensor data into actionable insights. This exemplifies STAG’s ability to refine raw data into a format ideal for practical applications.

5 Evaluation

We present a thorough evaluation of STAG, comparing it against established methods like InertiEar [14] and Stealthy-IMU. We focus on assessing STAG’s performance through a structured setup involving data bifurcation, training, testing, and key metrics like WER, SER, and SEER. This detailed analysis aims to validate STAG’s effectiveness and highlight its advancements in sensor data analysis for mobile devices.

5.1 Evaluation Setup

Our evaluation of STAG is conducted through a well-defined process, as depicted in Figure 6 that provides a comprehensive visual representation of the methodological framework adopted for assessing the system’s effectiveness.

5.1.1 Down sampling and bifurcation: To assess STAG’s predictive accuracy, we first established a ground truth by standardizing the dataset we collected earlier, originally sampled between 400 Hz and 500 Hz, downsampled to 400 Hz. This ensures compatibility with STAG’s upscaling capabilities. We then split the sensor readings into alternating (odd and even) samples to emulate an accelerometer operating at a reduced 200 Hz rate, aligning with STAG’s operational scenario. Odd accelerometer and even gyroscope samples were used for STAG input, with even accelerometer samples set aside as feedback for the training model discussed in Section 5.1.2.

This bifurcation mimics STAG’s enhancement process for an under-sampled accelerometer. The dataset was divided into training (70%), validation (15%), and testing (15%) subsets to optimize and test the LightGBM model’s performance within STAG, ensuring the model learns from complex patterns for precise predictions. Specifically, the dataset consisted of 36,000 samples, with 25,200 samples in the training set, 5,400 samples in the validation set, and 5,400 samples in the test set.

5.1.2 Training: During this phase, the training subset undergoes preprocessing steps like noise reduction and Z-score normalization. These steps prepare the data for processing by the LightGBM algorithm. The training phase is divided into two parts. First, we train a LightGBM model with odd accelerometer values as features and even accelerometer values as feedback. This itself gives us a good baseline, as seen in Figure 5(a). After the model is trained, we carry out cubic spline interpolation on odd accelerometer values, combining the output of the interpolation with the one from the model to train a new combined model. We use mean squared error and R-squared to finetune our model.

Hyperparameter tuning was performed using a grid search method, combined with 5-fold cross-validation on the training set, to ensure the selected hyperparameters generalized well. The best hyperparameters were chosen based on performance on the validation set.

To mitigate concerns about overfitting with the LightGBM model, we employed careful data partitioning and cross-validation throughout our evaluation, demonstrating the robustness and generalizability of our approach.

5.1.3 Testing: The testing subset, subjected to similar preprocessing, is input into the already trained LightGBM model. Here, the algorithm estimates the missing accelerometer samples. These predictions are then merged with the outputs from cubic spline interpolation and further refined through a subsequent application of LightGBM. This dual-phase processing with LightGBM ensures refined accuracy in the system’s final output. The final resulting output can be seen in Figure 5(c). The testing resulted in an average R-squared of 0.58.

5.2 Evaluation Metrics

To thoroughly assess the performance of STAG, we employ the following metrics:

- **Word Error Rate (WER):** This metric is widely used in automatic speech recognition (ASR) to gauge the accuracy of speech recognition systems. WER calculation is based on the Levenshtein distance, a measure that quantifies the difference between two sequences of letters, which, in this case, represent words in a transcription. Adjustments involving substitution, deletion, or insertion of words are made to align the recognized word sequence with the ground truth. WER is expressed as the ratio of the total number of

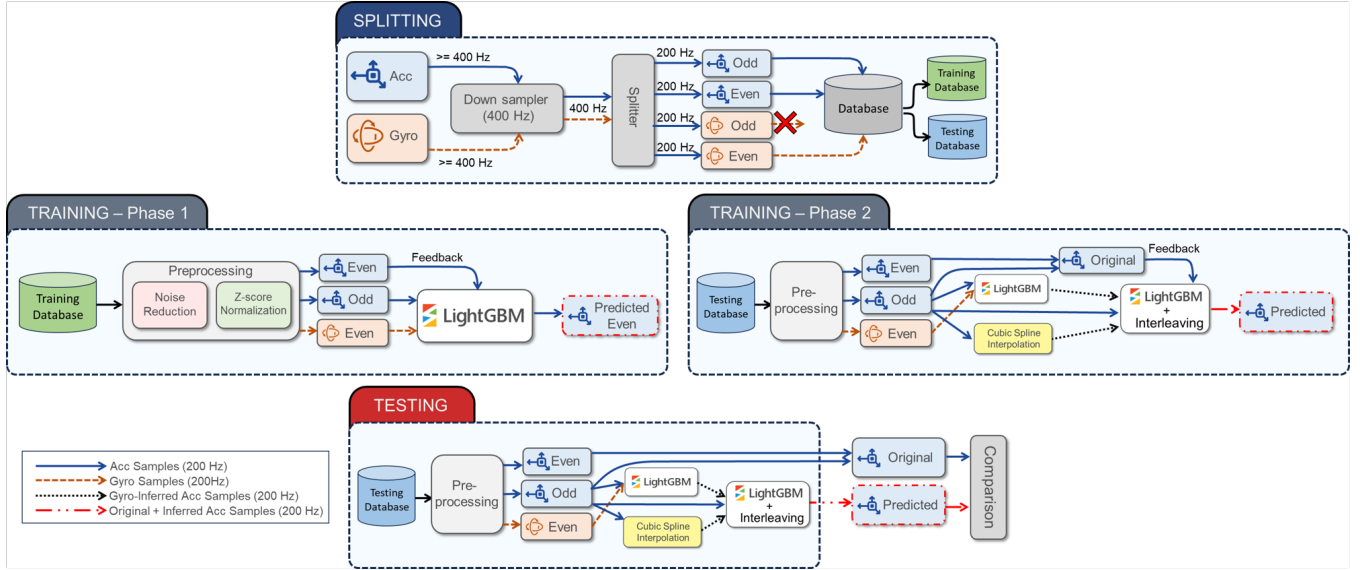


Figure 6. The STAG evaluation process: highlighting data downsampling, bifurcation, and model training/testing phases.

errors (substitutions, deletions, and insertions) to the total number of words in the standard word sequence [31]:

$$WER = \frac{D + S + I}{N} \times 100 \quad (1)$$

Here, D , S , I , and N denote the number of deletions, substitutions, insertions, and total words in the standard word sequence, respectively.

- **Sentence Error Rate (SER):** This metric is used to evaluate the accuracy of SLU responses. SER considers a response to be error-free only if all entities in a single voice assistant response are correctly identified. It is a comprehensive measure for evaluating the accuracy of SLU responses and is calculated as SER is:

$$SER = \frac{\# \text{ Incorrect Sentences}}{\text{Total Sentences}} \quad (2)$$

- **Single Entity Error Rate (SEER):** In SLU, a single voice assistant response may contain multiple entities. SEER is akin to WER but focuses on the entities within SLU responses. It measures the accuracy of identifying individual entities as follows:

$$SEER = \frac{\# \text{ Incorrect Entities}}{\text{Total Entities}} \quad (3)$$

These metrics provide a comprehensive framework for evaluating the effectiveness of STAG in both speech recognition and understanding contexts, enabling a holistic assessment of the system's performance.

5.3 Results

We now comparatively analyze STAG's performance against two established approaches in SLU applications: *InertiEar* [14] and *StealthyIMU* [29]. Our discussion is anchored by the key results detailed in Table 4, showcasing STAG's WER of

13% and SEER of 20%. These metrics underscore the general accuracy in transcribing function words and also the STAG's adeptness at capturing semantically significant entities such as names and locations. This performance is significantly better than that of *StealthyIMU* and *InertiEar*, suggesting an enhanced capability for dealing with complex audio data.

StealthyIMU relies solely on accelerometer data without integrating gyroscope data, limiting its ability to recognize complex speech patterns effectively. In contrast, *InertiEar* attempts to utilize both accelerometer and gyroscope data. However, their methodology largely involves using temporally aligned sensor data, which does not significantly enhance accuracy due to the minimal temporal disparity between the data streams. This alignment results in suboptimal performance as the interleaving of synchronized data provides no substantial improvement over using single sensor data.

STAG distinguishes itself by employing a novel method of inducing deliberate temporal misalignment between accelerometer and gyroscope data. This strategic misalignment allows STAG to exploit the unique data characteristics of each sensor type more effectively, significantly enhancing the system's ability to decode complex audio signals. By shifting the data streams in time, STAG achieves a higher fidelity in reconstructing speech, demonstrated by superior WER and SEER results. Also, as detailed in Section 4.2, STAG leverages the high SNR of the accelerometer's Z-axis and intelligently combines it with the X and Y axes of the gyroscope, which are temporally misaligned. This approach not only optimizes SNR but also ensures a more meaningful correlation between the data streams, enhancing both the accuracy and reliability of the sensor data utilized by STAG.

Table 4. Results: STAG achieves 58% reduction in SER and an 86% decrease in WER, outperforming the other methods sampling data at 200 Hz.

	SER%	SEER%	WER%
StealthyIMU [29]	99.68	83.7	78.75
InertiEar [14]	84.94	42	24.44
STAG	42.83	21	13.02

This comparative analysis conclusively underlines the superiority of STAG’s methodology. By effectively harnessing the power of temporal misalignment, STAG advances the capabilities of SLU systems, outperforming traditional methods like those employed by *InertiEar* and *StealthyIMU*. The results validate the effectiveness of STAG and highlight its potential to redefine the landscape of sensor-based SLU technologies.

STAG showed remarkable improvements: a 58% reduction in sentence error rate and an 86% reduction in word error rate, compared to data sampled at 200 Hz without up-scaling.

6 Discussion

Countermeasures: To prevent the STAG-based zero-permission attack for unauthorized speech recognition, several countermeasures can be implemented. First, imposing stricter access controls on motion sensor data can significantly reduce the risk of exploitation. This includes requiring explicit user permissions for accessing accelerometer and gyroscope data, even at lower sampling rates. This measure ensures that only authorized applications can access sensitive sensor data, thereby protecting user privacy.

Another effective measure would be to employ noise injection techniques, which add benign noise to sensor readings. This approach obfuscates the data, rendering it less useful for precise speech recognition without significantly degrading the performance of legitimate applications that rely on sensor data.

Finally, configuring the magnetometer and IMU to be directly connected to the host, rather than as a slave, would help mitigate the issue. In this setup, the magnetometer interrupts would not affect the FIFO buffer within the IMU, as they would be handled by the host instead.

By addressing these potential vulnerabilities and implementing robust countermeasures, the risk of unauthorized speech recognition via STAG can be significantly mitigated. These measures ensure better protection of user privacy while maintaining the functionality and performance of authorized applications.

Outlook: As Android continues to evolve, upcoming versions are likely to include improvements in sensor data handling and synchronization, which could prevent the temporal misalignment exploit utilized by STAG. While our findings reflect the system’s present state, they underscore the importance of

implementing a timely security patch. By raising awareness of this issue now, we aim to encourage proactive steps to safeguard user privacy.

The current implementation of STAG leverages the Stealthy-IMU SLU model, which is optimized for English. This presents an opportunity to integrate more advanced and multilingual SLU models, such as those developed in recent advancements [6, 32]. Incorporating these models will improve accuracy and also extend STAG’s utility to multilingual contexts, making it accessible and effective across different cultural and linguistic settings.

Another exciting challenge is optimizing STAG’s signal processing algorithms to run on-device, reducing dependency on internet connectivity. By processing data locally, STAG can operate efficiently even in environments with limited connectivity. This optimization will also address concerns related to data storage and transmission, as on-device processing can store only speech recognition outputs, which are significantly smaller than raw sensor data. This approach will enhance user privacy and reduce data storage requirements.

7 Conclusion

We introduced STAG, a novel approach designed to circumvent the limitations imposed by Android’s 200 Hz sampling rate cap on IMU sensors. By inducing a temporal misalignment between the gyroscope and accelerometer, and leveraging sophisticated data fusion techniques, STAG achieves a significant reduction in word error rate (86%), demonstrating a robust capability to enhance acoustic surveillance under restricted conditions. The proposed method showcases a technical advancement in exploiting IMU data and highlights the need for more stringent security measures in smartphone sensors.

Our evaluation provides compelling evidence of STAG’s ability to manipulate sensor data to overcome existing security protocols, which were thought to mitigate such risks. The approach underscores the persistent vulnerabilities in smartphone sensor security and serves as a critical reminder of the ongoing need for advancements in this area to protect user privacy.

References

- [1] spaCy · Industrial-strength Natural Language Processing in Python — spacy.io. <https://spacy.io/>. (????). [Accessed 20-04-2024].
- [2] Types of voices | Cloud Text-to-Speech API | Google Cloud — cloud.google.com. <https://cloud.google.com/text-to-speech/docs/voice-types>. (????). [Accessed 24-06-2024].
- [3] 2024. StealthyIMU VUI dataset. (2024). <https://drive.google.com/file/d/18wBg8mehJZ0gLW6O8T7fkq53J-8EQLdJ/view?usp=sharing> Accessed: 2024-06-20.
- [4] S Abhishek Anand and Nitesh Saxena. 2018. Speechless: Analyzing the Threat to Speech Privacy from Smartphone Motion Sensors. In *2018 IEEE Symposium on Security and Privacy (SP)*. 1000–1017. <https://doi.org/10.1109/SP.2018.00004>
- [5] S Abhishek Anand, Chen Wang, Jian Liu, Nitesh Saxena, and Yingying Chen. 2021. Spearphone: A Lightweight Speech Privacy Exploit via

Accelerometer-Sensed Reverberations from Smartphone Loudspeakers. In *Proceedings of the 14th ACM Conference on Security and Privacy in Wireless and Mobile Networks (WiSec '21)*. Association for Computing Machinery, New York, NY, USA, 288–299. <https://doi.org/10.1145/3448300.3468499>

[6] Siddhant Arora, Hayato Futami, Jee-weon Jung, Yifan Peng, Roshan Sharma, Yosuke Kashiwagi, Emiru Tsunoo, and Shinji Watanabe. 2023. Universlu: Universal spoken language understanding for diverse classification and sequence generation tasks with a single network. *arXiv preprint arXiv:2310.02973* (2023).

[7] Author. 2024. (2024).

[8] V. Kishore Ayyadevara. 2018. *Gradient Boosting Machine*. Apress, Berkeley, CA, 117–134. <https://doi.org/10.1007/978-1-4842-3564-56>

[9] Zhongjie Ba, Tianhang Zheng, Xinyu Zhang, Zhan Qin, Baochun Li, Xue Liu, and Kui Ren. 2020. Learning-based Practical Smartphone Eavesdropping with Built-in Accelerometer.. In *NDSS*, Vol. 2020. 1–18. <https://doi.org/10.14722/ndss.2020.24076>

[10] BOSCH. 2024. BMI160 Datasheet. <https://www.bosch-sensortec.com/media/bosch-sensortec/downloads/datasheets/bst-bmi160-ds000.pdf>. (2024). [Accessed 19-04-2024].

[11] R.E. Crochiere and L.R. Rabiner. 1981. Interpolation and decimation of digital signals—A tutorial review. *Proc. IEEE* 69, 3 (1981), 300–331. <https://doi.org/10.1109/PROC.1981.11969>

[12] Anupam Das, Gunes Acar, Nikita Borisov, and Amogh Pradeep. 2018. The Web’s Sixth Sense: A Study of Scripts Accessing Smartphone Sensors. In *Proceedings of the 25th ACM Conference on Computer and Communication Security (CCS)*. ACM. <https://doi.org/10.1145/3243734.3243860>

[13] Wilfried Elmenreich. 2002. An introduction to sensor fusion. *Vienna University of Technology, Austria* 502 (2002), 1–28.

[14] Ming Gao, Yajie Liu, Yike Chen, Yimin Li, Zhongjie Ba, Xian Xu, and Jinsong Han. 2022. InertiEAR: Automatic and Device-independent IMU-based Eavesdropping on Smartphones. In *IEEE INFOCOM 2022 - IEEE Conference on Computer Communications*. 1129–1138. <https://doi.org/10.1109/INFOCOM48880.2022.9796890>

[15] Google. 2013. Manage your Android device’s location settings - Android Help. (2013). <https://support.google.com/android/answer/3467281?sjid=16509926452287363758-EU> [Accessed 03-12-2023].

[16] Google. 2023. Behavior changes: Apps targeting Android 12. (2023). <https://developer.android.com/about/versions/12/behavior-changes-12#motion-sensor-rate-limiting> [Accessed 02-12-2023].

[17] Jun Han, Albert Jin Chung, and Patrick Tague. 2017. PitchIn: Eavesdropping via Intelligible Speech Reconstruction Using Non-acoustic Sensor Fusion. In *2017 16th ACM/IEEE International Conference on Information Processing in Sensor Networks (IPSN)*. 181–192.

[18] Pengfei Hu, Hui Zhuang, Panneer Selvam Santhalingam, Riccardo Spolaor, Parth Pathak, Guoming Zhang, and Xiuzhen Cheng. 2022. AccEar: Accelerometer Acoustic Eavesdropping with Unconstrained Vocabulary. In *2022 IEEE Symposium on Security and Privacy (SP)*. 1757–1773. <https://doi.org/10.1109/SP46214.2022.9833716>

[19] Guolin Ke, Qi Meng, Thomas Finley, Taifeng Wang, Wei Chen, Weidong Ma, Qiwei Ye, and Tie-Yan Liu. 2017. LightGBM: A Highly Efficient Gradient Boosting Decision Tree. In *Advances in Neural Information Processing Systems*, I. Guyon, U. Von Luxburg, S. Bengio, H. Wallach, R. Fergus, S. Vishwanathan, and R. Garnett (Eds.), Vol. 30. Curran Associates, Inc.

[20] Kazusuke Maenaka. 2008. MEMS inertial sensors and their applications. In *2008 5th International Conference on Networked Sensing Systems*. IEEE, 71–73.

[21] Yan Michalevsky, Dan Boneh, and Gabi Nakibly. 2014. Gyrophone: Recognizing Speech from Gyroscope Signals. In *23rd USENIX Security Symposium (USENIX Security 14)*. USENIX Association, San Diego, CA, 1053–1067. <https://www.usenix.org/conference/usenixsecurity14/technical-sessions/presentation/michalevsky>

[22] Alexey Natekin and Alois Knoll. 2013. Gradient boosting machines, a tutorial. *Frontiers in Neurorobotics* 7 (2013). <https://doi.org/10.3389/fnbot.2013.00021>

[23] Emmanuel Owusu, Jun Han, Sauvik Das, Adrian Perrig, and Joy Zhang. 2012. ACCesory: Password Inference Using Accelerometers on Smartphones. In *Proceedings of the Twelfth Workshop on Mobile Computing Systems & Applications (HotMobile '12)*. Association for Computing Machinery, New York, NY, USA, Article 9, 6 pages. <https://doi.org/10.1145/2162081.2162095>

[24] John H Ryalls and Philip Lieberman. 1982. Fundamental frequency and vowel perception. *The Journal of the Acoustical Society of America* 72, 5 (1982), 1631–1634.

[25] J.Z. Sasiadek. 2002. Sensor fusion. *Annual Reviews in Control* 26, 2 (2002), 203–228. [https://doi.org/10.1016/S1367-5788\(02\)00045-7](https://doi.org/10.1016/S1367-5788(02)00045-7)

[26] Jurek Z Sasiadek. 2002. Sensor fusion. *Annual Reviews in Control* 26, 2 (2002), 203–228.

[27] Derek K. Shaeffer. 2013. MEMS inertial sensors: A tutorial overview. *IEEE Communications Magazine* 51, 4 (2013), 100–109. <https://doi.org/10.1109/MCOM.2013.6495768>

[28] ST. 2024. LSM6DSL Datasheet. <https://www.st.com/resource/en/datasheet/lsm6dsl.pdf>. (2024). [Accessed 19-04-2024].

[29] Ke Sun, Chunyu Xia, Songlin Xu, and Xinyu Zhang. 2023. StealthyIMU: Stealing Permission-protected Private Information From Smartphone Voice Assistant Using Zero-Permission Sensors. <https://doi.org/10.14722/ndss.2023.24077>

[30] LO Thielman, S Bennett, CH Barker, and ME Ash. 2002. Proposed IEEE Coriolis Vibratory Gyro standard and other inertial sensor standards. In *2002 IEEE Position Location and Navigation Symposium (IEEE Cat. No. 02CH37284)*. IEEE, 351–358.

[31] Thilo von Neumann, Christoph Boeddeker, Keisuke Kinoshita, Marc Delcroix, and Reinhold Haeb-Umbach. 2023. On Word Error Rate Definitions and Their Efficient Computation for Multi-Speaker Speech Recognition Systems. In *ICASSP 2023 - 2023 IEEE International Conference on Acoustics, Speech and Signal Processing (ICASSP)*. 1–5. <https://doi.org/10.1109/ICASSP49357.2023.10094784>

[32] Minghan Wang, Yinglu Li, Jiaxin Guo, Xiaosong Qiao, Zongyao Li, Hengchao Shang, Daimeng Wei, Shimin Tao, Min Zhang, and Hao Yang. 2023. Whislu: End-to-end spoken language understanding with whisper. In *Proc. Interspeech*, Vol. 2023. 770–774.

[33] Ye-Yi Wang, Li Deng, and A. Acero. 2005. Spoken language understanding. *IEEE Signal Processing Magazine* 22, 5 (2005), 16–31. <https://doi.org/10.1109/MSP.2005.1511821>

[34] Mitchell Webber and Raul Fernandez Rojas. 2021. Human activity recognition with accelerometer and gyroscope: A data fusion approach. *IEEE Sensors Journal* 21, 15 (2021), 16979–16989.

[35] Ja-Woong Yoon, Yeon-Sik Noh, Yi-Suk Kwon, Won-Ki Kim, and Hyung-Ro Yoon. 2014. Improvement of dynamic respiration monitoring through sensor fusion of accelerometer and gyro-sensor. *Journal of Electrical Engineering and Technology* 9, 1 (2014), 334–343.

[36] Li Zhang, Parth H. Pathak, Muchen Wu, Yixin Zhao, and Prasant Mohapatra. 2015. AccelWord: Energy Efficient Hotword Detection through Accelerometer. In *Proceedings of the 13th Annual International Conference on Mobile Systems, Applications, and Services (MobiSys '15)*. Association for Computing Machinery, New York, NY, USA, 301–315. <https://doi.org/10.1145/2742647.2742658>